Monte Carlo Simulation of Post-Wildfire Flood Hazard Probabilities

Jeremy Giovando, Research Hydraulic Engineer, USACE ERDC-CRREL, Hanover, NH, Jeremy.J.Giovando@usace.army.mil

Kathryn Seefus, Hydraulic Engineer, USACE Omaha District, Omaha, NE, kathryn.j.seefus@usace.army.mil

Evan Heisman, Hydraulic Engineer, USACE IWR-HEC, Davis, CA, evan.a.heisman@usace.army.mil

Extended Abstract

Wildfires are a significant natural hazard (Kim & Jakus, 2019) and are increasing in size in recent decades (Dennison et al., 2014; Westerling et al., 2006; Westerling, 2016; Yang et al., 2015). A consequence of the increased wildfire activity is changes to runoff into streams and rivers which has been investigated in several publications. Annual flow volume increases of 20%-200% have been reported (Hallema et al., 2018; Niemeyer et al., 2020; Wine et al., 2018). These changes can persist for several decades (Niemeyer et al. 2020). In addition to volume changes, the post-wildfire peak flow magnitude can also be enhanced substantially. Studies have reported several orders of magnitude increase for post-wildfire peak flows (Coombs & Melack, 2013; Ice et al., 2004; Neary, 2002; Neary et al., 2003, 2010; Scott & Van Wyk, 1990).

Many communities in the US regulate development in the floodplain based on peak flow probabilities (e.g. 1 % annual exceedance probability (AEP)). The challenge for local and state agencies is the peak flow probabilities are often based on pre-wildfire watershed conditions and there is limited information or guidance about how to adjust the peak flow magnitudes following the wildfire disturbance. The most recent study identified which uses observed peak flow changes in burned watersheds across the western US was by Yu et al. (2022). They reported that the median post-wildfire peak flows were increased relative to pre-wildfire period for watersheds with at least 25% of the drainage area burned.

The objective of our analysis is to develop a framework that can be used to quantitatively estimate post-wildfire flow frequency changes. To accomplish this objective we used two software tools from the Hydrologic Engineering Center (HEC). These tools include the Hydrologic Modeling System (HEC-HMS) and the Watershed Analysis Tool (HEC-WAT), which includes a stochastic event generator for Monte Carlo simulations, called Hydrologic Sampler (HS). We tested this framework on the Cache La Poudre (CLP) Basin in northern Colorado which was recently impacted by the Cameron Peak Fire in 2020. The CLP River is a snowmelt dominated stream with peak flows occurring during the May through June period.

Methods

Modeling Framework

The overall modeling framework consisted of development and calibration of an HEC-HMS model for the CLP Basin. The calibration was performed on four pre-wildfire snowmelt runoff events (April through June) with 24-hour precipitation greater than 1 inch. There is limited historical flow data available for calibration; therefore the primary data used was at the Canyon Mouth gage (Figure 1). The daily flows have regulation and trans-basin diversions removed to

provide as close to a naturalized flow value as possible. The Monte Carlo simulation consisted of 15,000 events using a combination of precipitation depths, storm shapes, temperature sequences, and initial snowpack conditions. To create the data needed for the Monte Carlo simulation several tasks were performed. This included a precipitation frequency analysis along with a storm shape analysis were used to disaggregate randomly sampled precipitation totals from the HS. In addition, a set of several air temperature sequences for each subbasin were used as input and are based on historical air temperature data. The set air temperature sequences were derived from extracting average daily air temperature during large precipitation events during the April through June season.

Using a historical snow water equivalent (SWE) reanalysis dataset developed by Broxton et al. (2019), a spatially averaged daily SWE time series for mountainous regions (Figure 1) was derived. The time series was then subset to only include daily values from March through May. This subset SWE data time series was then ordered by percentile ranking. To create the set of initial SWE values for each subbasin within the HEC-WAT, the mountainous region SWE was sampled 250 times on equal intervals across the range of percentiles. Then using a bootstrap sampling method the SWE values were disaggregated to individual subbasins by selecting the individual subbasin SWE values for the subset of days that had a mountainous region SWE equal to the 250 sampled values; therefore ensuring that each set of SWE values was representative of the spatial distribution for each subbasin. For example if the mountainous region SWE was 6 inches depth, then all daily SWE distributions that had an average 6 inch depth for the mountainous region average were pooled together. The pooled SWE distributions between subbasins were then sampled using a bootstrap method to create the spatially disaggregated SWE for each subbasin used in the HEC-HMS model[1].

The Monte Carlo simulation of these events was then simulated in HEC-WAT by HEC-HMS with each hydrologic event using a unique combination of precipitation depth, initial snowpack, and air temperature to produce peak flow values at the Canyon Mouth streamgage (Figure 1). The ensemble output of events provides direct calculation of confidence limits on the flow frequency distribution. These limits include combined uncertainty of precipitation, temperature, initial snowpack, and parameterization values.

The relative differences between pre- and post-wildfire flow frequency produced by the Monte Carlo simulation was used to adjust the pre-wildfire flow frequency curve developed using systematic data records and Bulletin 17c methods (England et al. 2018).

---

[1] R code for this process can be obtained from the authors at https:// http://github.com/eheisman/BootstrapSWE
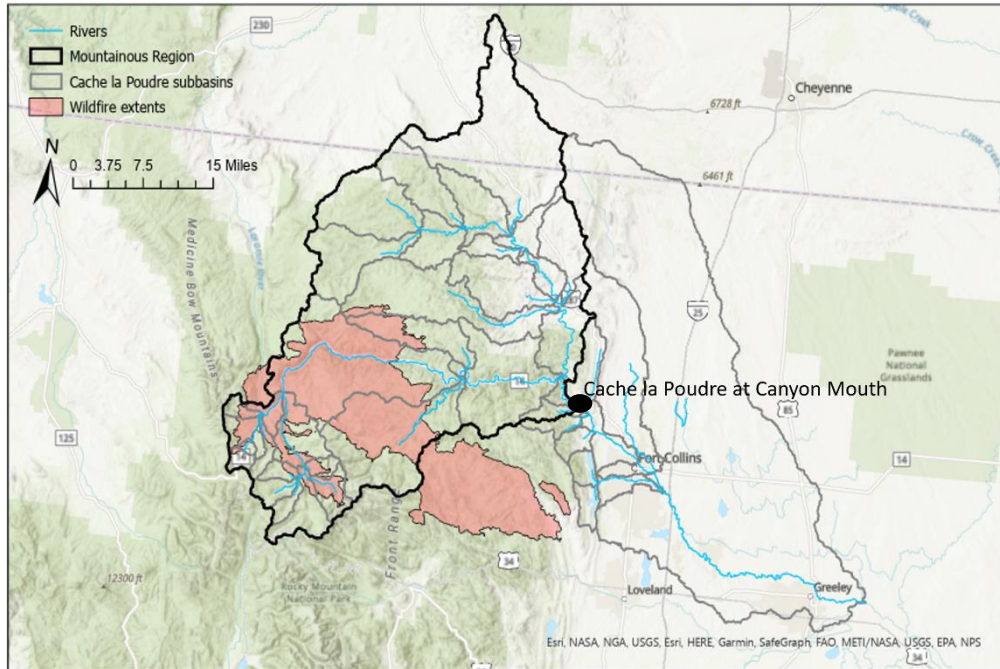
Figure 1: CLP Basin in northern Colorado. The Cameron Peak Fire burn perimeter (orange) impacted large areas of the upper watershed. The primary HEC-HMS calibration location was at the Canyon Mouth streamgage.

Precipitation Frequency

Forcing data for the HEC-HMS model was derived from the Analysis of Record for Calibration precipitation and temperature data (AORC) (Kim & Villarini 2022). This data is one hour temporal resolution and 4 km spatial resolution for the continuous US. We aggregated to total precipitation over 24-hours and extracted the annual maximum precipitation values. Using these values, we developed the precipitation frequency quantiles for the CLP Basin (Figure 2). Both temperature and precipitation temporal distributions, at the subbasin level, were developed from the AORC data. Eight precipitation events and the corresponding temperatures, primarily occurring in May and greater than the 20% AEP, were chosen to represent the storm shapes. By using different temporal distributions of hourly forcing data, this provides a better estimate of confidence limits at each AEP.
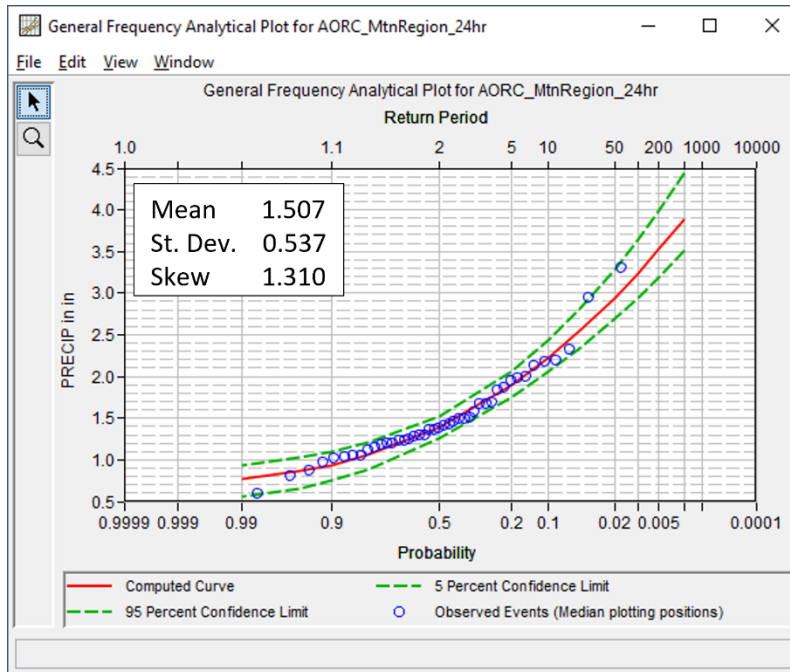
Figure 2: 24-hour precipitation frequency curve based on the AORC hourly data and used as input to the Hydrologic Sampler tool in HEC-WAT.

HEC-HMS Model Parameter Adjustments

The pre-wildfire calibration was used to set the parameters for the CLP HEC-HMS model. For the post-wildfire parameters, the burn severity and extents from two relatively recent fires in the CLP were used for adjustments. The parameter adjustments were performed for areas that were burned either in the 2012 High Park or 2020 Cameron Peak fires were. Parameter adjustments for the combined area were used because vegetation recovery following the High Park Fire has been minimal. Many of the forested areas burned in 2012 are now grass and small shrubs. We assumed areas which did not get impacted by wildfire were still represented by the pre-wildfire parameter set. In addition, only the infiltration, canopy interception, and snowmelt parameters were adjusted for the burned parts of the CLP. Other parameters required for routing water off the hillslope and through the channel network remained unchanged from the pre-wildfire calibration.

For areas that did burn, the parameter adjustments were based on those found in the literature. The reduction of infiltration has been reported in several publications (Ebel et al., 2012; Ebel & Moody, 2017, 2020; Moody & Martin, 2001, 2015; Neary et al., 2010). Using the values reported in Ebel & Moody (2020) a 63% reduction in infiltration was applied to the pre-wildfire saturated hydraulic conductivity parameters in HEC-HMS. The final saturated hydraulic conductivity for burned subbasins was weighted for each burned subbasin by applying the 63% reduction to burn areas with moderate or high burn severity and combining that with the pre-wildfire saturated hydraulic conductivity for the remain area which was low burn severity or unburned. Parameter uncertainty can be directly included in HEC-HMS and is input as a range within the user interface. The pre-wildfire range of saturated hydraulic conductivity was 0.27 to 1.50, while the post-wildfire range was 0.10 to 1.50.

In addition, snowmelt rates were included in the parameter uncertainty within HEC-HMS. The pre-wildfire melt-rates ranged from 0.04 to 0.12. The post-wildfire snowmelt rate was adjusted to 0.04 to 0.20 which are 5% to 200% higher than pre-wildfire rates. The melt-rate adjustments are based on analysis of SNOTEL sites in Colorado which have been impacted by wildfire and measurements from Burles & Boon (2011).

Results

The frequency curve shown in Figure 3 was developed from the pre-wildfire annual maximum peak flow events using the guidelines for flow frequency described in England et al. (2018). The plotting positions of the systematic events are based on the entire 1990-2012 dataset. Figure 4 is a comparison of the HEC-WAT pre- and post-wildfire frequency curves for the CLP at Canyon Mouth. The relative difference between these curves ranges from 247 cfs at the 50% ACE to 5,262 cfs at 0.2% ACE.

The relative difference was applied to the pre-wildfire frequency curve to obtain the post-wildfire frequency curve as seen in Figure 5. The post-wildfire years are also overplotted with the pre-wildfire frequency curve. Based on applying the relative differences determined through the Monte Carlo simulations, the post-wildfire increase in peak flow values is approximately equal to the upper confidence limit of the pre-wildfire flow frequency estimate for probabilities less than 60%.

We did perform the Monte Carlo simulation using only the 2012 High Park effects and the combined effects from both fires. The flow frequency differences compared to pre-wildfire values were minimal using only the High Park fire effects. The combined High Park and Cameron Peak fire effects resulted in much larger peak flow differences between pre- and post-wildfire conditions.
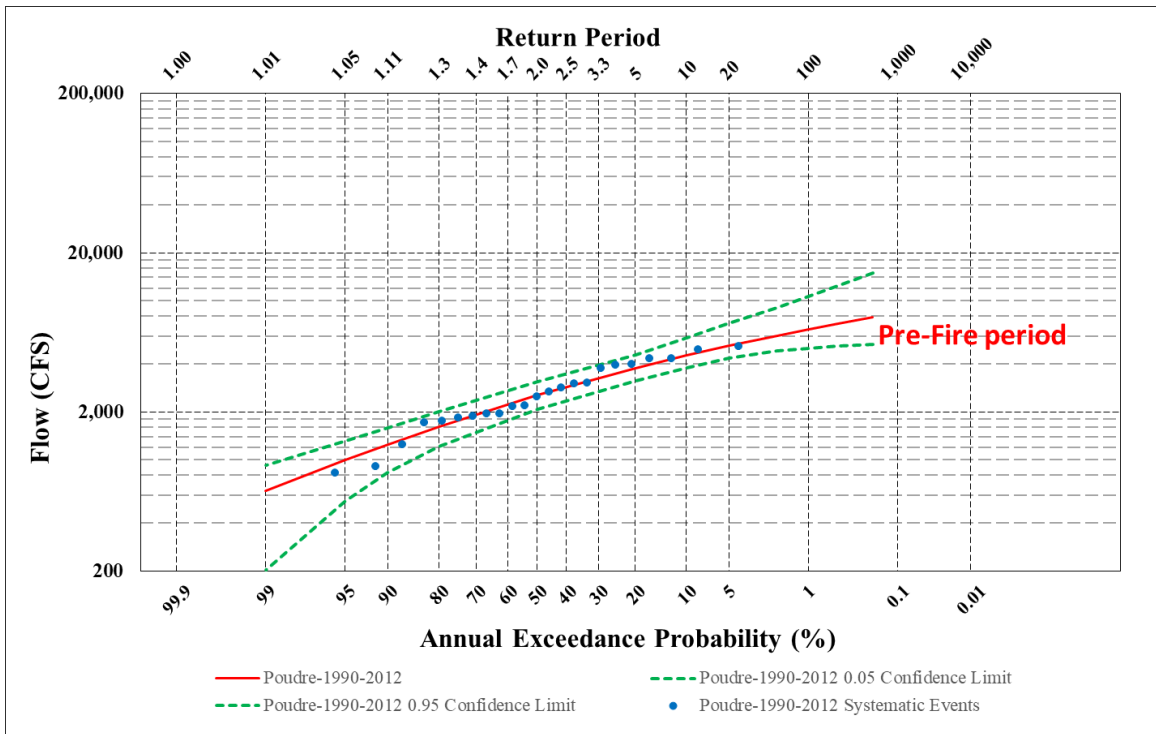
Figure 3: CLP at Canyon Mouth pre-wildfire peak flow frequency curve based naturalized flow 1990-2012 using USGS Bulletin 17c procedures (England et al. 2018).
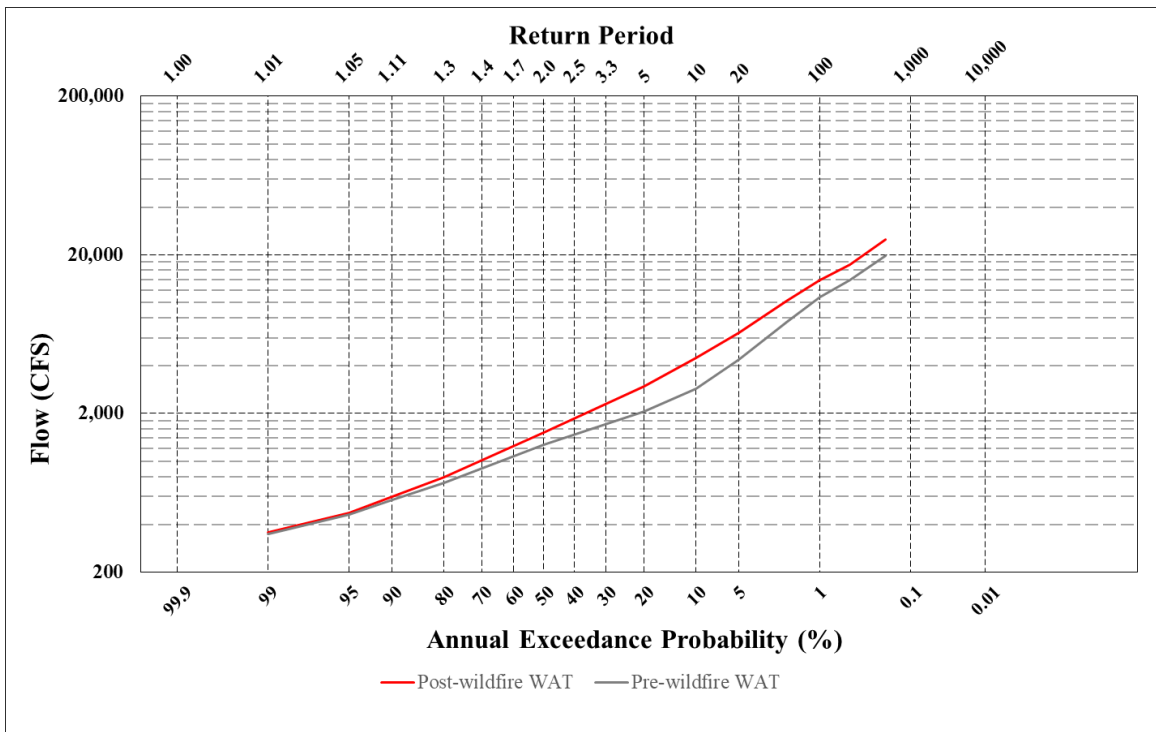

Figure 4: Monte Carlo simulation results using HEC-WAT and HEC-HMS for CLP at Canyon Mouth peak flow frequency curves. Pre-wildfire results (grey) and post-wildfire results (red).
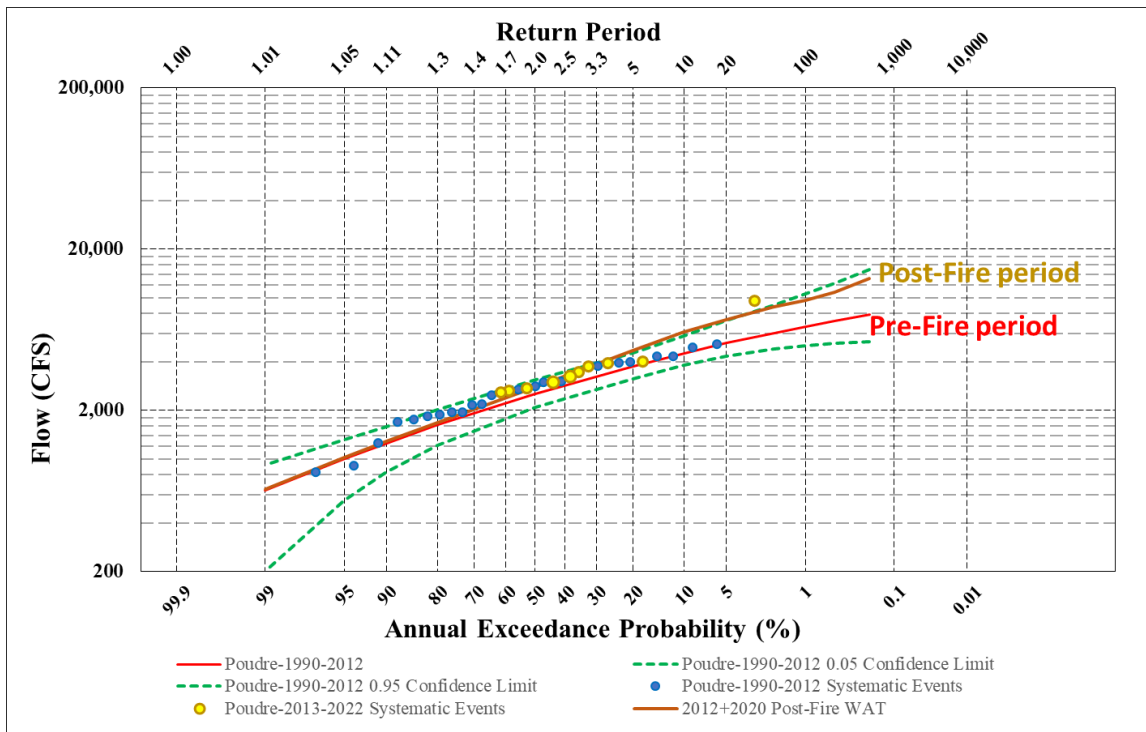
Figure 5: Comparison of the systematic pre- and post-wildfire frequency curves using relative difference produced by the Monte Carlo simulation.

Conclusions

Based on the literature, post-wildfire increases in peak flow values are expected for rainfall events, however changes to snowmelt and rainfall runoff events have not been investigated nearly to the same extent. There are several key limitations to our analysis including limited historical streamflow data locations, the number of calibration years available that included large precipitation events, and assuming the effects of the 2012 High Park fire are still present. In addition, further refinements to the HEC-HMS model can be made to better capture peak flow events during dryer years. Our results indicated that peak flow changes for higher probabilities (lower peak flow values) do not substantially change from pre- to post-wildfire. Further investigation into these results should occur to ensure this is not an artifact of the model parameterization. A potential solution may be to create a pre- and post-wildfire parameter set specifically for years with lower peak flow values. This could then be combined with the results from our current analysis to provide better definition for the full range of probabilities.

The framework we have described uses publicly available software tools and can be used on most any high-end personal computer. In addition, our process allows for direct quantification of uncertainty associated with input variables (i.e., temperature, precipitation, and initial snowpack) and hydrologic model parameters (e.g., saturated hydraulic conductivity, melt-rate, etc.). Finally, by using pre-wildfire information to calibrate an HEC-HMS model and Monte Carlo simulations, we have provided a process which can be used by state and local officials during the post-wildfire recovery period to assess changes in flood risk to communities and critical infrastructure.

References

Burles, K. and Boon, S. (2011), Snowmelt energy balance in a burned forest plot, Crowsnest Pass, Alberta, Canada. Hydrol. Process., 25: 3012-3029. https://doi.org/10.1002/hyp.8067

Broxton, P., X. Zeng, and N. Dawson. (2019). Daily 4 km Gridded SWE and Snow Depth from Assimilated In-Situ and Modeled Data over the Conterminous US, Version 1 [Data Set]. Boulder, Colorado USA. NASA National Snow and Ice Data Center Distributed Active Archive Center. https://doi.org/10.5067/0GGPB220EX6A. Date Accessed 06-03-2022.

Coombs, J. S., & Melack, J. M. (2013). Initial impacts of a wildfire on hydrology and suspended sediment and nutrient export in California chaparral watersheds. *Hydrological Processes*, *27*(26), 3842–3851. https://doi.org/10.1002/hyp.9508

Dennison, P. E., Brewer, S. C., Arnold, J. D., & Moritz, M. A. (2014). Large wildfire trends in the western United States, 1984-2011. *Geophys. Res. Lett.*, *41*, 2928–2933.

Ebel, B. A., & Moody, J. A. (2017). Synthesis of soil-hydraulic properties and infiltration timescales in wildfire-affected soils. *Hydrological Processes*, *31*(2), 324–340. https://doi.org/10.1002/hyp.10998

Ebel, B. A., & Moody, J. A. (2020). *Parameter estimation for multiple post-wildfire hydrologic models*. *July*, 4049–4066. https://doi.org/10.1002/hyp.13865

Ebel, B. A., Moody, J. A., & Martin, D. A. (2012). Hydrologic conditions controlling runoff generation immediately after wildfire. *Water Resources Research*, *48*(3), 1–13. https://doi.org/10.1029/2011WR011470

England, J.F., Jr., Cohn, T.A., Faber, B.A., Stedinger, J.R., Thomas, W.O., Jr., Veilleux, A.G., Kiang, J.E., and Mason, R.R., Jr. (2018). Guidelines for determining flood flow frequency—Bulletin 17C (ver. 1.1, May 2019): U.S. Geological Survey Techniques and Methods, book 4, chap. B5, 148 p., https://doi.org/10.3133/tm4B5.

Hallema, D. W., Sun, G., Caldwell, P. V., Norman, S. P., Cohen, E. C., Liu, Y., Bladon, K. D., & McNulty, S. G. (2018). Burned forests impact water supplies. *Nature Communications*, *9*(1), 1–8. https://doi.org/10.1038/s41467-018-03735-6

Ice, G. G., Neary, D. G., & Adams, P. W. (2004). Effects of Wildfire on Processes. *Journal of Forestry*, *102*(September), 16–20.

Kim, H., & Villarini, G. (2022). Evaluation of the Analysis of Record for Calibration (AORC) Rainfall across Louisiana. *Remote Sensing*, *14*(14). https://doi.org/10.3390/rs14143284

Kim, M. K., & Jakus, P. M. (2019). Wildfire, national park visitation, and changes in regional economic activity. *Journal of Outdoor Recreation and Tourism*, *26*(February 2018), 34–42. https://doi.org/10.1016/j.jort.2019.03.007

Moody, J. A., & Martin, D. A. (2001). Post-fire, rainfall intensity-peak discharge relations for three

mountainous watersheds in the Western USA. *Hydrological Processes*, *15*(15), 2981–2993. https://doi.org/10.1002/hyp.386

Moody, J. A., & Martin, R. G. (2015). Measurements of the initiation of post-wildfire runoff during rainstorms using in situ overland flow detectors. *Earth Surface Processes and Landforms*, *40*(8), 1043–1056. https://doi.org/10.1002/esp.3704

Neary, D. G. (2002). Post-Wildfire Flood Generation Processes. *Hydrology and Water Resources in Arizona and the Southwest*, *32*.

Neary, D. G., Gottfried, G. J., & Ffolliott, P. F. (2003). Post-Wildfire Watershed Flood Responses. *Second International Fire Ecology and Fire Management Congress, Orlando, Florida, 16-20 November 2003, Paper 1B7*, 1–8.

Neary, D. G., Koestner, K. A., & Youberg, A. (2010). Hydrologic Impacts of High Severity Wildfire : Learning from the Past and Preparing for the Future. *24th Annual Symposium of the Arizona Hydrological Society; Watersheds near and Far: Response to Changes in Climate and Landscape*, 8. http://www.fs.fed.us/rm/pubs_other/rmrs_2011_neary_d003.pdf?

Niemeyer, R. J., Bladon, K. D., & Woodsmith, R. D. (2020). Long-term hydrologic recovery after wildfire and post-fire forest management in the interior Pacific Northwest. *Hydrological Processes*, *34*(5), 1182–1197. https://doi.org/10.1002/hyp.13665

Scott, D. F., & Van Wyk, D. B. (1990). The effects of wildfire on soil wettability and hydrological behaviour of an afforested catchment. *Journal of Hydrology*, *121*(1–4), 239–256. https://doi.org/10.1016/0022-1694(90)90234-O

Westerling, A. L., Hidalgo, H. G., Cayan, D. R., & Swetnam, T. W. (2006). Warming and earlier spring increase western US forest wildfire activity. *Science*, *313*(5789), 940–943. https://doi.org/10.1126/science.1128834

Westerling, A. L. R. (2016). Increasing western US forest wildfire activity: Sensitivity to changes in the timing of spring. *Philosophical Transactions of the Royal Society B: Biological Sciences*, *371*(1696). https://doi.org/10.1098/rstb.2015.0178

Wine, M. L., Makhnin, O., & Cadol, D. (2018). Nonlinear Long-Term Large Watershed Hydrologic Response to Wildfire and Climatic Dynamics Locally Increases Water Yields. *Earth's Future*, *6*(7), 997–1006. https://doi.org/10.1029/2018EF000930

Yang, J., Tian, H., Tao, B., Ren, W., Pan, S., Liu, Y., & Wang, Y. (2015). A growing importance of large fires in conterminous United States during 1984-2012. *Journal of Geophysical Research: Biogeosciences*, *120*(12), 2625–2640. https://doi.org/10.1002/2015JG002965